Redox Biology 54 (2022) 102390

Contents lists available at ScienceDirect

Redox Biology

journal homepage: www.elsevier.com/locate/redox

Adiponectin/AdiopR1 signaling prevents mitochondrial dysfunction and oxidative injury after traumatic brain injury in a SIRT3 dependent manner

Shenghao Zhang [1], Xun Wu [1], Jin Wang [1], Yingwu Shi, Qing Hu, Wenxing Cui, Hao Bai, Jinpeng Zhou, Yong Du, Liying Han, Leiyang Li, Dayun Feng, Shunnan Ge [**], Yan Qu [*]

Department of Neurosurgery and Institute for Functional Brain Disorders, Tangdu Hospital, Fourth Military Medical University, Xi'an, 710038, China

ARTICLE INFO

Keywords:
TBI
APN
SIRT3
Oxidative stress
Mitochondria

ABSTRACT

Mitochondrial dysfunction and oxidative injury, which contribute to worsening of neurological deficits and poor clinical outcomes, are hallmarks of secondary brain injury after TBI. Adiponectin (APN), beyond its well-established regulatory effects on metabolism, is also essential for maintaining normal brain functions by binding APN receptors that are ubiquitously expressed in the brain. Currently, the significance of the APN/APN receptor (AdipoR) signaling pathway in secondary injury after TBI and the specific mechanisms have not been conclusively determined. In this study, we found that APN knockout aggravated brain functional deficits, increased brain edema and lesion volume, and exacerbated oxidative stress as well as apoptosis after TBI. These effects were significantly alleviated after APN receptor agonist (AdipoRon) treatment. Moreover, we found that AdipoR1, rather than AdipoR2, mediated the protective effects of APN/AdipoR signaling against oxidative stress and brain injury after TBI. In neuron-specific AdipoR1 knockout mice, mitochondrial damage was more severe after TBI, indicating a potential association between APN/AdipoR1 signaling inactivation and mitochondrial damage. Mechanistically, neuron-specific knockout of SIRT3, the most important deacetylase in the mitochondria, reversed the neuroprotective effects of AdipoRon after TBI. Then, PRDX3, a critical antioxidant enzyme in the mitochondria, was identified as a vital downstream target of the APN/SIRT3 axis to alleviate oxidative injury after TBI. Finally, we revealed that APN/AdipoR1 signaling promotes SIRT3 transcription by activating the AMPK-PGC pathway. In conclusion, APN/AdipoR1 signaling plays a protective role in post-TBI oxidative damage by restoring the SIRT3-mediated mitochondrial homeostasis and antioxidant system.

1. Introduction

Globally, traumatic brain injury (TBI), a leading cause of morbidity and mortality [1–3], is associated with a heavy burden on patients and society [4,5]. Moreover, an effective treatment option for TBI is lacking [6]. Typically, mitochondrial injury and oxidative damage occur following TBI [7,8], and they cause persistent damage to brain tissues. Thus, clarifying its occurrence mechanism and establishing the targeted intervention strategy are critical for encountering deleterious pathophysiological insults after TBI.

Adiponectin (APN), a 30 kDa cytokine solely produced by differentiated adipocytes (i.e., adipocytokine), plays crucial roles in modulating numerous physiological processes by binding to its specific receptors [9–11]. APN has multiple biological effects, such as anti-oxidative stress, anti-inflammatory and anti-apoptotic properties [12–15]. The levels of adiponectin are paradoxically decreased with increasing adiposity and various of pathologies, including type 2 diabetes, metabolic syndrome, and atherosclerosis [16,17]. Clinical and population-based studies support an association between APN and CNS diseases [18–20]. For instance, low circulating adiponectin levels are associated with poor functional outcomes following an ischemic stroke [19,20]. Furthermore, supplementary of APN confers neuroprotective effects on intracerebral hemorrhage (ICH), vascular dementia and Alzheimer's disease [13,21,22]. Biologically, APN exerts its central and peripheral effects by binding two different APN transmembrane receptors; adiponectin receptor type 1 (AdipoR1), and adiponectin receptor type 2 (AdipoR2) [23,24]. AdipoR1 selectively activates the AMP-activated kinase (AMPK) pathway, while AdipoR2 exerts its biological effects by activating the

* Corresponding author.
** Corresponding author.
E-mail addresses: gesn8561@fmmu.edu.cn (S. Ge), yanqu0123@fmmu.edu.cn (Y. Qu).
[1] These authors contributed equally to this work.

https://doi.org/10.1016/j.redox.2022.102390
Received 30 May 2022; Received in revised form 24 June 2022; Accepted 28 June 2022
Available online 30 June 2022

PPARα pathway [25]. AdipoRon, a small molecule agonist of APN receptors, can selectively activate both AdipoR1 and AdipoR2 [26,27], which can readily penetrate the blood-brain barrier (BBB) and exert the same effects as those of APN in the CNS [26,28]. This provides a promising prospective towards clinical translation of the mechanism involved in APN-associated anti-oxidative stress and opens up opportunities for clinical applications in CNS diseases. However, the effects of APN on oxidative stress following TBI and its potential mechanisms have not been explored.

It is acknowledged that APN shows promising therapeutical effects on mitochondrial dysfunction which is a vital trigger of oxidative stress [13,22,29,30], but the underlying mechanisms have not been fully clarified. Sirtuin 3 (SIRT3), the major NAD^+-dependent deacetylase, is exclusively located in the mitochondria and is expressed in tissues with high mitochondrial content, such as brain tissues [31]. It possesses potent deacetylase activity toward a set of metabolic targets, including electron transport chain complex subunits and enzymes involved in redox balance, fatty acid oxidation and the tricarboxylic acid cycle (TCA) [32]. Previous researches have indicated that multiple enzymes central to mitochondrial antioxidative defense system are modified by lysine acetylation, and many of them are hyperacetylated in the absence of SIRT3. SIRT3 deficiency may lead to the dysfunction of antioxidant protein, resulting in excess ROS generation and induction of oxidative stress [33–39]. Hence, SIRT3 is considered as a vital regulator of mitochondrial functions, antioxidative defense systems and energy metabolism [40–46]. Previous studies have indicated SIRT3 as a potential therapeutic target of TBI [47,48], while the relevant molecular mechanisms remain largely unexplored, restricting the establishment of treatment strategies.

In this study, we for the first time explored the role of the APN/AdipoR signaling in secondary brain injury after TBI and undercover a novel mechanism that APN prevents mitochondrial dysfunction and oxidative injury after traumatic brain injury in a SIRT3 dependent manner.

2. Methods

2.1. Experimental animals

The Fourth Military Medical University's ethical committee approved this study. All experimental procedures were in accordance with the National Institute of Health guidelines for the use of experimental animals. Adult healthy, 8-week-old male C57BL/6J mice weighing 20 g–25 g were purchased from the animal center of the Fourth Military Medical University. The $SIRT3^{flox/flox}$ mice were purchased from Jackson Laboratory (ME, USA), $APN^{-/-}$, $AdipoR1^{flox/flox}$ and MAP2-Cre ERT2 mice were generated in Shanghai Model Organisms Center, Inc (Shanghai, China). Mice were placed in a pathogen-free SPF animal room within an animal care facility, with constant temperature (23 °C), humidity (60%), 12-h light/dark cycle and allowed free access to food and water. Neuron-specific SIRT3 conditional knockout ($SIRT3^{CKO}$) and AdipoR1 conditional knockout ($AdipoR1^{CKO}$) mice were generated via $SIRT3^{flox/flox}$ mice or $AdipoR1^{flox/flox}$ mice with MAP2-Cre ERT2 mice. To induce conditional knockout of AdipoR1 and SIRT3 in the neurons, tamoxifen (75 mg/kg; 10,540, Sigma) was intraperitoneally administered daily for five days. Transgenic mice were identified by polymerase chain reaction analysis of genomic DNA in the tail using the following primers: for APN knockout: (5′- GGCTCTCTGGGAGAGGCGAGT - 3′), (5′- CCATCACGGCCTGGTGTGCC - 3′) and (5′- TTCGCCATTCAGGCTGCGCA - 3′); for AdipoR1 floxed: (5′- CGAGCCTACCTGGAGTTGAAGAGC - 3′) and (5′- GGGAAACCGCACTGAAGAGAACCT - 3′); for SIRT3 floxed: (5′- CTGGCT TTGGGTTTAAGCAG - 3′) and (5′- GGAGGCTGAGGCTAAAGAGC - 3′); for Cre: (5′- GCATCACCCCGACGACTCAG - 3′), (5′- GTATTGGATAGCCTTCAGGCAC - 3′) and (5′- GGTGTTATAAGCAATCCCCAGAA - 3′). PCR results were visualized on 1.2% agarose gel.

2.2. Establishment of TBI mice models and drug treatment

Induction of TBI in mice was as described earlier [49,50]. Anesthesia was induced in mice via intraperitoneal injection of pentobarbital sodium (60 mg/kg). Mice were subjected to moderate controlled cortical impact (CCI) brain injuries with a unilateral of 1.6 mm depth at 2.5 m/s and 300 ms dwell time using the microprocessor-controlled pneumatic impacting device (RWD Life Science, Shenzhen China) with a 3.5 mm diameter tip. The craniotomies were located midway between the bregma and lambda suture on the right side of the brain. Mice were rewarmed in a cage at an ambient temperature of 37 °C for 1 h. The surgical site was cleaned using ethanol. The sham operation group was only subjected to right parietal craniotomy. All operations were aseptically performed. AdipoRon (HY-15848, MedChemExpress, New Jersey, USA) was dissolved in 1% DMSO/PBS after which animals were randomly assigned to receive intraperitoneal injections of AdipoRon (5 mg/kg body weight) [28] or an equivalent volume of the vehicle at 0.5 h after TBI.

2.3. Measurement of the cerebral lesion volume

A 3T small animal MRI scanner (Bruker MRI GmbH, Germany) was used to produce mice brain images. Mice were anesthetized using 10% chloral hydrate and placed in dorsal recumbency over an MRI-compatible holder as previously described [51]. Cerebral structural data were acquired using the MRI scanner with a radiofrequency surface and phased array mouse brain coil. To calculate the cerebral lesion volume, MRI images were exported in a DICOM format and analyzed by ImageJ.

2.4. Determination of water content in brain tissues

Brain moisture contents were measured using the wet-dry weight ratio method as previously described [52]. The ratio was as: Brain tissue moisture content (%) = (wet weight-dry weight)/wet brain weight × 100%.

2.5. DHE staining

As mentioned previously [53], ROS levels were evaluated by DHE (Yesen) and MitoSOX (Invitrogen) staining. After anesthesia, mice brain tissues were collected and frozen at −80°Cfor 20 min. Then, they were quickly sliced into coronal sections (15 μm thick), which were incubated in DHE (10 μmol/L) for 30 min. Primary neurons were incubated in DHE (10 μmol/L) for 30 min at room temperature. Finally, slices and cells were examined and imaged by confocal laser scanning microscopy (Nikon, A1Si, Japan). Relative fluorescence levels of ROS were quantified by ImageJ.

2.6. TUNEL staining

TUNEL staining was performed to assess apoptosis levels, as instructed by the kit manufacturer (Roche). Briefly, we treated samples with 0.3% hydrogen peroxide for 30 min and incubated them for 45 min in the presence of protease K. After that, samples were immersed in a solution of TUNEL reaction for 60 min. Finally, DAPI (Invitrogen) was used to label the samples, and the ratio of TUNEL-positive cells to DAPI-stained cells was calculated to determine the degree of apoptosis.

2.7. Neurological function assessment

Twenty-four hours after CCI, the modified neurological severity score (mNSS) test was blindly performed by a researcher in the experimental group, as mentioned earlier [29]. The mNSS score was 0–18 (normal score was 0, highest defect score was 18). This test consists of movement, sensation, balance and reflex tests. The higher the score, the

more serious the injury.

In the corner turn test [49], mice approached the 30° corner after which they could freely exit the corner either by turning to the right or left. The percentage of a left turns in 10 trials was calculated.

In the wire hanging test [54], a metal wire (50 cm) was stretched between two posts and suspended 50 cm above the ground. Mice were guided to grasp the wire with their forelimbs. Medical adhesive tape was applied to their hindlimbs to prevent them from using them. When mice were properly suspended, they were allowed to hang by themselves. Then, we measured the latency to fall, the time less than 10 s was excluded from analysis.

2.8. Transmission electron microscopy

Sample preparation was performed as previously described [29]. Briefly, 24 h after TBI, mice were anesthetized and perfused as usual. Their brains were removed and placed in ice-cold Hanks' Balanced Salt Solution. Each brain was sliced into 1 mm-thick sections in the coronal position. The cortical sample (1×2 mm^2) was selected and fixed overnight in 4% glutaraldehyde at 4 °C. After 1 h of fixation in 1% osmium tetroxide, by using graded ethanol series, the slices were dehydrated, then resin-embedded. Embedded sample blocks were trimmed and sliced by an ultra-thin slicer, after which slices were placed on 200-slot grids coated with a pioloform membrane and imaged by JEM-1400 electron microscopy (JEOL, Tokyo, Japan) and a charge coupled device camera (OLYPUS, Tokyo, Japan).

2.9. Primary neuron cultures and adenovirus-mediated shRNA and Cre treatment

Primary neurons were isolated from C57 mice embryos as previously described [55]. Briefly, primary cortical brains were removed from C57 mice embryos and digested with a trypsin solution. Mixed cells were plated in F12 medium supplemented with 1% L-glutamate, 10% fetal bovine serum (Gibco), as well as 1% double antibiotics (Gibco) and incubated in a 5% CO_2/95% atmosphere for 4 h (37 °C). Then, the neurobasal medium with 2% B27, 1% L-glutamine and 1% double antibiotics (Gibco) was used to replace the F12 medium. Half-replacement of the medium was done every 3 days. At 3–4 days after plating, the addition of cytosine arabinoside was conducted to inhibit glial proliferation. To determine the effects of PRDX3, AdipoR1 and AdipoR2, adenovirus vector U6/CMV-GFP shRNA (1×10^9 PFU/mL, GenePharma, China) targeting PRDX3, AdipoR1 and AdipoR2 were generated and administered to respectively knock down PRDX3, AdipoR1 and AdipoR2. Primary cortical neurons from SIRT3$^{flox/flox}$ mice were transfected with Ad5CMVCre-eGFP (Ad-Cre-GFP) (1×10^9 PFU/mL, GenePharma, China) to generate SIRT3^{CKO} primary neurons [56].

2.10. Scratch injury model and AdipoRon treatment

A previously described scratch injury method was used to establish *in vitro* TBI models [57]. Briefly, primary neurons were manually scratched using sterile pipette tips (10 μl), which generated a linear injury across the cell surface, after which they were treated with the vehicle or 50 μM AdipoRon for 24 h. The space between each scratch was about 3 mm. The culture was incubated without changing the culture medium. The control group was not subjected to any intervention.

2.11. MitoSOX staining

Mitochondrial ROS levels were detected using MitoSOX™ Red (Invitrogen). The MitoSOX Red reagent is oxidized by superoxide in the mitochondria, exhibiting a red fluorescence [58]. Primary neurons were incubated in MitoSOX (5 nmol/L) for 30 min and washed twice using warm HBSS. Fluorescent images were imaged by confocal laser scanning microscopy (Nikon, A1Si, Japan) and analyzed using ImageJ.

2.12. Determination of ATP, MDA and activities of antioxidant enzymes

At 24 h after TBI, mice were sacrificed, their tissues obtained, lysed using a lysis buffer (Beyotime, Jiangsu, China) and homogenized for 30 min on ice. Supernatants were obtained after centrifugation (12,000 rpm) of samples for 10 min at 4 °C. Malondialdehyde (MDA) (Beyotime, Jiangsu, China), ATP (Beyotime, Jiangsu, China) levels and activities of oxidative stress-related enzymes, MnSOD (Beyotime, Jiangsu, China) and GSH-Px (Beyotime, Jiangsu, China) were assessed as instructed by the manufacturers' corresponding commercial kits.

2.13. Measurement of mitochondrial respiratory chain complex activities

A Mitochondria/Cytosol Fractioning Kit (Solarbio, Beijing, China) was used to isolate the mitochondria and cytosol, as instructed by the manufacturer. Briefly, samples were washed twice using ice-cold PBS and thereafter resuspended in 500 μl of extraction buffer containing protease inhibitors on ice for 10 min. Samples were homogenized using a Dunce grinder and centrifuged at 800 g for 10 min at 4 °C. Precipitations were discarded and supernatants centrifuged at 12,000 g for 20 min at 4 °C. Resulting supernatants were collected as cytosolic fractions after which pellets were dissolved in 50 μl lysis buffer to obtain the mitochondrial fraction. Activities of mitochondrial respiratory chain complexes I, II, III, IV and V were measured using the corresponding kits (Solarbio, Beijing, China), as instructed by the manufacturer.

2.14. Quantitative real-time PCR

Total RNA from brain tissues and primary neuron samples from each group were extracted using the Trizol RNA isolation kit (15,596–018, Invitrogen, USA), as instructed by the manufacturer. Then, cDNA was synthesized from total RNA for each sample using appropriate primers, according to the Invitrogen protocol. The SIRT3 primers were (5′-CCCAGTGGCATTCCAGACTT - 3′) and (5′-AAGGGCTTGGGGTTGT-GAAA-3′). The β-actin primers were (5′-CTGGCACCCAGCACAATG-3′) and (5′-GTTCATGAGGCACACCTAGCC-3′). RT-qPCR was performed in a 10 μL reaction system containing cDNA, forward/reverse primers, and SYBR Green ReadyMix (Fisher Scientific, Atlanta, USA). Relative expressions of RNAs were computed by $2^{-\triangle\triangle Ct}$ method.

2.15. Immunoprecipitation and Co-IP

Cell samples were harvested in a lysis buffer containing a proteinase inhibitor mixture at 4 °C for 4 h. After centrifugation at 4 °C (13,000 rpm) for 10 min, the supernatant was obtained and incubated in the presence of *anti*-SIRT3 (10,099, Proteintech) or *anti*-PRDX3 (ab264354, Abcam) or non-specific IgG overnight at 4 °C. Then, 40 μl protein A/G magnetic beads (MedchemExpress, NJ, USA) were added to the mixture and incubated at room temperature for 4 h. A magnetic rack was used to capture the beads, which were washed thrice using a Co-IP lysis buffer and resolved in a loading buffer to be prepared for Western blotting.

2.16. Western blotting

Samples from brain tissues and cultured cells were lysed, homogenized in an ice-cold lysis buffer containing protease inhibitors and phosphatase for 20 min and sonicated. A SDS-PAGE was used to separate proteins and the separated proteins were transferred onto PVDF membranes (Millipore, USA). The membranes were immersed in 5% non-fat milk for 2 h and incubated at 4 °C overnight in the presence of primary rabbit polyclonal antibodies against Bcl-2 (12,789, Proteintech), Bax (50,599, Proteintech), AMPK (66,536, Proteintech), p-AMPK (2537, CST), PGC-1α (66,369, Proteintech), SIRT3 (10,099, Proteintech), PRDX3 (ab264354, Abcam), acetylated-Lysine (9441, CST), VDAC (55,259, Proteintech), and β-actin (AC026, ABclonal). Then, membranes were incubated for 2 h with corresponding HRP-conjugated secondary

antibodies (AS003, AS014, ABclonal) at room temperature. Protein bands were captured by a Bio-Rad Imaging System (Bio-Rad, USA) and analyzed using the ImageJ software.

2.17. Statistical analysis

GraphPad Prism 8 (GraphPad Software Inc, USA) was used for statistical analyses. Unless otherwise stated, values are expressed as mean ± standard deviation (SD). A two-tailed Student's t-test was used to assess differences in means between groups while one-way analysis of variance (ANOVA) followed by the Tukey's post hoc test was used to assess differences among groups. $p \leq 0.05$ was the threshold for statistical significance.

3. Results

3.1. APN deficiency exacerbated lesion volume, brain edema and neurological functional deficits after TBI

First, APN knockout mice were used to evaluate the potential role of APN/AdipoR signaling in brain injury after TBI. Validation of APN knockout are presented in the identification results (Fig. 1A). By measuring lesion volume, brain water contents, we found that APN deficiency significantly increased TBI-induced cerebral lesion volumes (Fig. 1B and C) and exacerbated brain edema (Fig. 1D). We also assessed the neurological functions. The results showed that APN deficiency significantly increased the mNSS score after TBI (Fig. 1E) and was also associated with poor performance in the wire-hanging and corner turn tests after TBI (Fig. 1F and G). The above results indicate that APN deficiency exacerbates the organic and functional damage of brain after

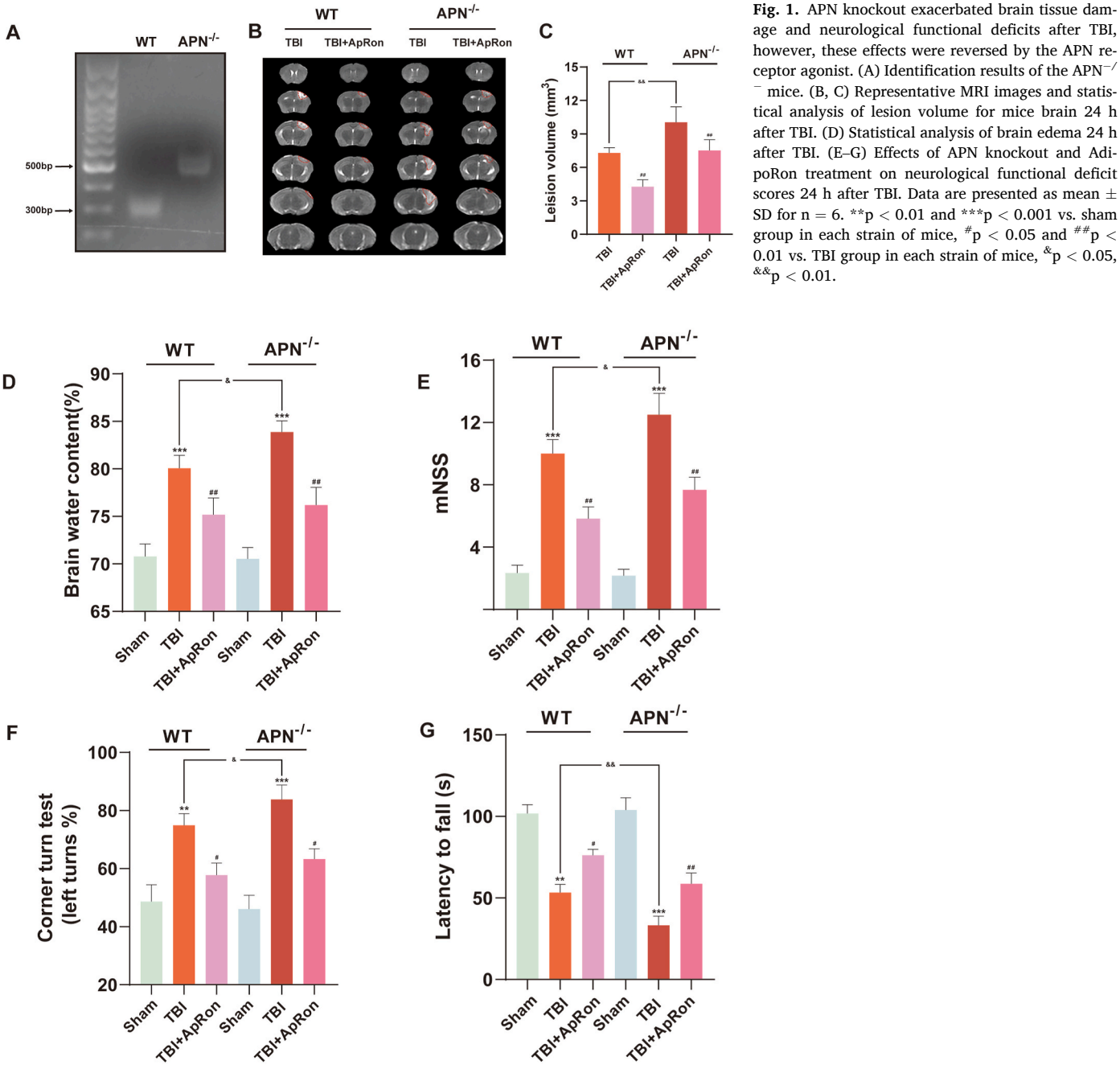

Fig. 1. APN knockout exacerbated brain tissue damage and neurological functional deficits after TBI, however, these effects were reversed by the APN receptor agonist. (A) Identification results of the $APN^{-/-}$ mice. (B, C) Representative MRI images and statistical analysis of lesion volume for mice brain 24 h after TBI. (D) Statistical analysis of brain edema 24 h after TBI. (E–G) Effects of APN knockout and AdipoRon treatment on neurological functional deficit scores 24 h after TBI. Data are presented as mean ± SD for n = 6. $^{**}p < 0.01$ and $^{***}p < 0.001$ vs. sham group in each strain of mice, $^{\#}p < 0.05$ and $^{\#\#}p < 0.01$ vs. TBI group in each strain of mice, $^{\&}p < 0.05$, $^{\&\&}p < 0.01$.

TBI.

3.2. AdipoRon treatment reversed lesion volume, brain edema and neurological functional deficits after TBI

The APN receptor agonist (AdipoRon) was used to evaluate whether activation of APN/AdipoR signaling attenuates TBI-induced organic and functional damage of brain. The results showed that AdipoRon treatment could reduce the lesion volume (Fig. 1B and C) and alleviated brain edema (Fig. 1D) in both WT and APN$^{-/-}$ mice after TBI. For functional damage of brain after TBI, AdipoRon treatment could also respectively reversed the deteriorated evaluation of mNSS score, wire-hanging and corner turn tests in both mouse lines (Fig. 1E–G). These results demonstrate that APN has neuroprotective effects against TBI.

3.3. APN deficiency aggravated oxidative stress and neural apoptosis after TBI

Oxidative stress is a major cause of secondary injuries after TBI [13], thus we explored the effects of APN on oxidative stress. First, DHE staining was performed to determine ROS levels. In WT or APN$^{-/-}$ mice, DHE fluorescence density in TBI groups was markedly increased compared to sham groups, and a higher fluorescence density corresponded to increased ROS levels (Fig. 2A and B). Compared to WT mice, ROS levels were significantly higher in APN$^{-/-}$ mice after TBI (Fig. 2A and B). Moreover, the elevated MDA levels and suppressed MnSOD as well as GSH-Px activities in the perilesional cortex after TBI in APN$^{-/-}$ mice were more severe than those in WT mice (Fig. 2C–E). Excess ROS production induces neural apoptosis and contributes to deterioration of TBI [59,60]. Therefore, neural apoptosis was assessed by TUNEL staining. It was found that APN deletion increased the abundance of TUNEL-positive cells, compared to WT mice after TBI (Fig. 2F and G). Western blotting demonstrated that APN deficiency markedly aggravated the increase in Bax levels and decreased Bcl-2 levels after TBI, compared to WT mice (Fig. 2H–J). Therefore, the results indicate that APN deficiency aggravates oxidative stress and neural apoptosis after TBI.

3.4. AdipoRon treatment reversed the enhancement of oxidative stress and neural apoptosis after TBI

The elevated ROS levels in both WT and APN$^{-/-}$ mice were reversed

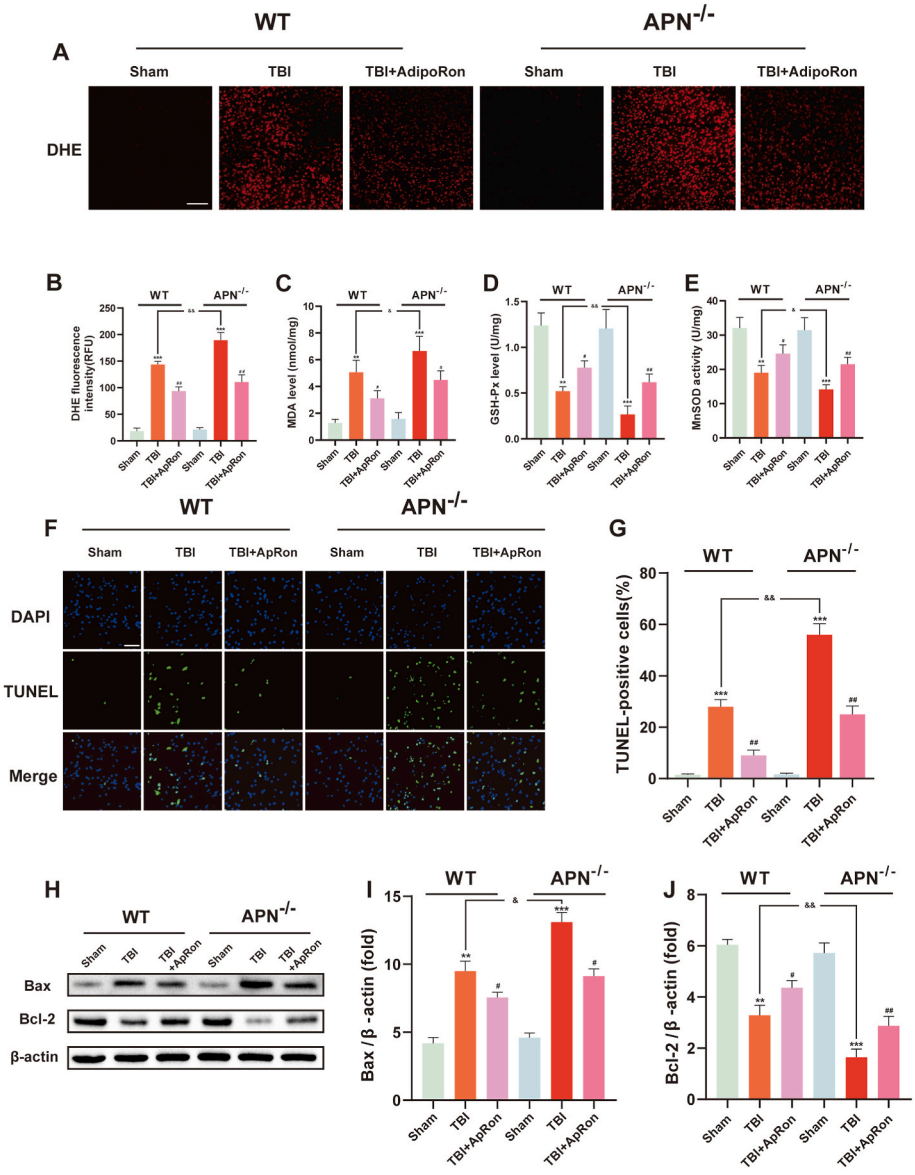

Fig. 2. APN knockout aggravated neural apoptosis and oxidative stress after TBI. APN receptor agonist alleviated the injury. (A, B) Typical images of DHE staining and statistical analysis of DHE fluorescence intensities of the perilesional cortex 24 h after TBI, which indicates ROS levels. Scale bar: 100 μm. (C–E) Effects of APN deficiency and AdipoRon treatment on MDA and GSH-Px levels as well as on MnSOD activities. (F, G) Representative images of TUNEL staining 24 h after TBI and corresponding statistical analysis. Scale bar: 100 μm. (H–J) Representative Western blot and statistical analysis of Bcl-2 and Bax protein levels. Data are presented as mean ± SD for n = 6. $^{**}p < 0.01$ and $^{***}p < 0.001$ vs sham group in each strain of mice, $^{\#}p < 0.05$ and $^{\#\#}p < 0.01$ vs TBI group in each strain of mice, $^{\&}p < 0.05$, $^{\&\&}p < 0.01$.

by AdipoRon treatment (Fig. 2A and B). Moreover, AdipoRon treatment could also reverse the elevated MDA levels and suppressed MnSOD as well as GSH-Px activities in the perilesional cortex after TBI in both mouse lines (Fig. 2C–E). Accordingly, AdipoRon treatment markedly reduced the increase in TUNEL-positive cells after TBI in both WT mice and APN$^{-/-}$ mice (Fig. 2F and G). Western blotting demonstrated that AdipoRon treatment could significantly reverse the increased Bax levels and decreased Bcl-2 levels after TBI (Fig. 2H–J). The results demonstrate that AdipoRon treatment could attenuate oxidative stress and neural apoptosis after TBI.

3.5. AdipoR1, rather than AdipoR2, mediated the protective effects of APN against TBI-induced oxidative stress and brain injury

To determine which APN receptor subtype mediates the protective effects of APN/AdipoR signaling against oxidative stress and brain injury after TBI, AdipoR1 and AdipoR2 in mouse cortical primary neurons were respectively knocked down using adenovirus (AV)-mediated shRNA. DHE fluorescence density results showed that AdipoRon activation effectively suppressed the ROS levels after scratching (Fig. 3A and B). This protective effect was abolished upon AdipoR1 knockdown, however, the protective effect remained after AdipoR2 knockdown (Fig. 3A and B). TUNEL staining revealed a reduced abundance of apoptotic cells when AdipoRon was applied after scratching, and AdipoR1 knockdown markedly abolished this protective effect, whereas, AdipoR2 knockdown could not exert the same effect (Fig. 3C and D). Given these findings, we generated neuron-specific AdipoR1 conditional knockout (AdipoR1^{CKO}) mice by crossing AdipoR1$^{flox/flox}$ mice with MAP2-creERT2 mice to further determine the protective effects of APN/AdipoR1 signaling in vivo (Fig. 3E and F). In mice, tamoxifen administration induced conditional knockout of AdipoR1 in neurons. Brain water content and neurological function assays revealed that AdipoR1 knockout significantly exacerbated the increase in brain water content and deteriorated neurological function after TBI (Fig. 3G–J). However, AdipoRon treatment could only reversed these adverse outcomes in AdipoR1$^{flox/flox}$ mice (Fig. 3G–J). These findings show that the protective effects of APN/AdipoR signaling against oxidative stress and brain injury are AdipoR1 dependent.

3.6. Neuron-specific AdipoR1 conditional knockout aggravated mitochondrial damage after TBI

We then evaluated the effects of AdipoR1 knockout on mitochondrial morphology and function after TBI. First, ultrastructural changes in

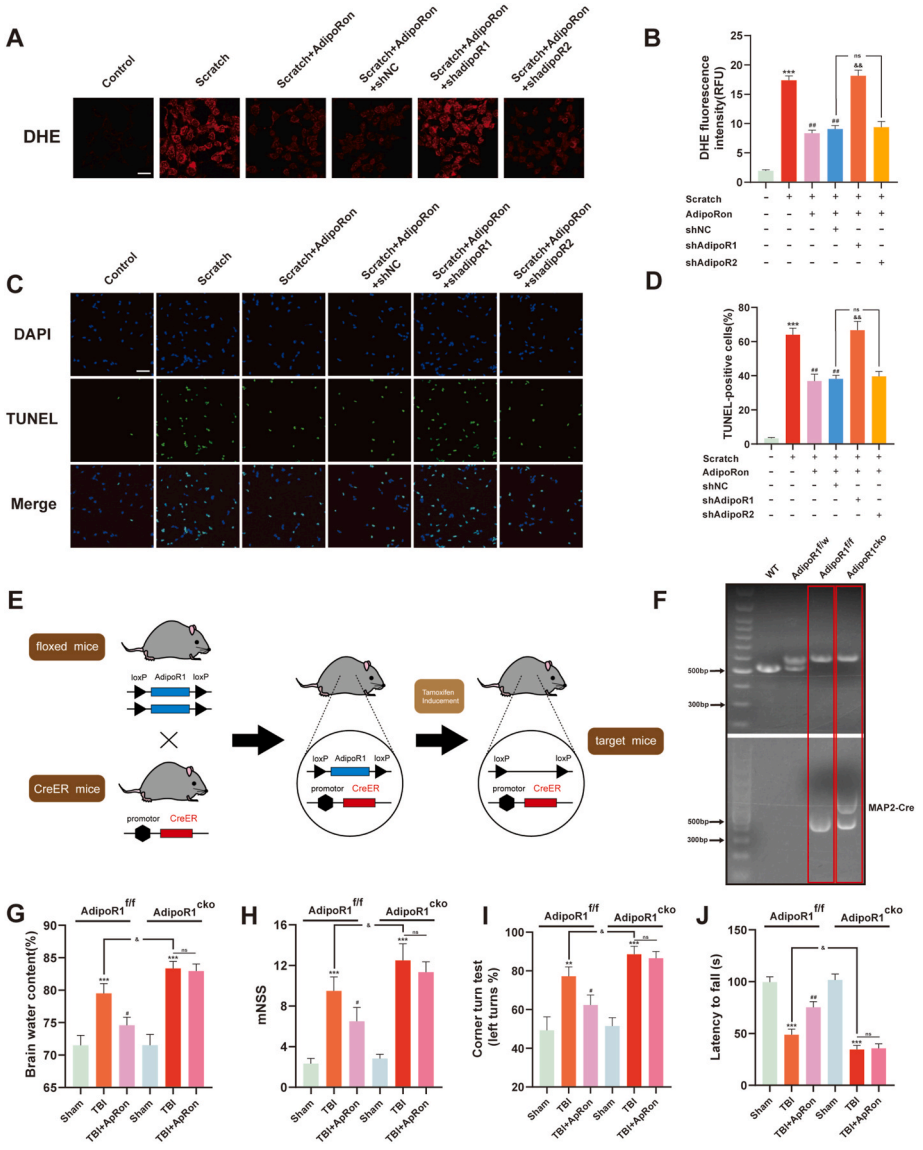

Fig. 3. AdipoR1 mediated the protective effects of APN/AdipoR signaling against oxidative stress and brain injury after TBI, while AdipoR2 could not. (A, B) Representative DHE images and statistical analysis of DHE fluorescence intensities for the effects of AdipoR1 or AdipoR2 knockdown on primary neurons 24 h after scratch, which indicates ROS levels. Scale bar: 50 μm. (C, D) Representative images and corresponding statistical analysis of TUNEL staining for the effects of AdipoR1 or AdipoR2 knockdown on primary neurons 24 h after scratch. Scale bar: 100 μm ***$p < 0.001$ vs control group, $^{\#\#}p < 0.01$ vs scratch group, $^{\&\&}p < 0.01$ vs scratch + AdipoRon + shNC group, ns: no statistical significance. (E) Diagram for construction of AdipoR1 conditional knockout mice. (F) Identification results of the neuron-specific AdipoR1 conditional knockout mice. (G–J) Effects of AdipoR1 knockout and AdipoRon treatment on brain edema and neurological function deficit scores 24 h after TBI. Data are presented as mean ± SD for n = 6. **$p < 0.01$ and ***$p < 0.001$ vs sham group in each strain of mice, $^{\#}p < 0.05$ and $^{\#\#}p < 0.01$ vs TBI group in each strain of mice, $^{\&}p < 0.05$, ns: no statistical significance.

neurons in response to TBI were observed on transmission electron micrographs, which revealed that mitochondrial damage was prominent after TBI in both AdipoR1$^{flox/flox}$ mice and AdipoR1^{CKO} mice, however, it was more severe in AdipoR1^{CKO} mice than in AdipoR1$^{flox/flox}$ mice (Fig. 4A). This was shown by mitochondrial swelling as well as the loss and disruption of mitochondrial cristae and mitochondrial membrane integrity. Therefore, we postulated that AdipoR1 is closely associated with the mitochondria. Further, we evaluated the mitochondrial function indicators and found that AdipoR1 knockout enhanced the decrease in ATP and mitochondrial respiratory chain complexes after TBI, compared to AdipoR1$^{flox/flox}$ mice (Fig. 4B–G). These results were consistent with the observation of mitochondrial morphology. Collectively, we found that AdipoR1 plays an important role in mitochondrial damage after TBI.

3.7. Neuron-specific SIRT3 conditional knockout reversed the protective effects of APN/AdipoR1 signaling activation on the mitochondria after TBI

The described results show that APN/AdipoR1 signaling has protective effects on the mitochondria. Therefore, we evaluated the specific mechanisms through which APN/AdipoR1 signaling regulates the mitochondria. SIRT3, a critical deacetylase that is primarily expressed in neurons, is exclusively located in the mitochondria [61]. It is involved in regulation of mitochondrial functions, metabolism, antioxidant defense systems and energy metabolism [61–63]. We found that AdipoR1 knockout exacerbates TBI-mediated decrease in SIRT3 transcription and expressions (Fig. 5A–C). AdipoRon treatment blocked the TBI-induced downregulation of transcription as well as expression of SIRT3 (Fig. 5D–F) and preserved its deacetylation activities in the mitochondria, as confirmed by increased SIRT3 protein levels and suppressed mitochondrial protein acetylation levels (Fig. 5G and H). To determine the role of AdipoRon treatment in SIRT3 mediated mitochondrial functions, we generated neuron-specific SIRT3 conditional knockout (SIRT3^{CKO}) mice by crossing SIRT3$^{flox/flox}$ mice with MAP2-creERT2 mice (Fig. 5I). Identification experiments were also performed (Fig. 5J). Transmission electron micrographs showed that the mitochondria from both SIRT3$^{flox/flox}$ mice and SIRT3^{CKO} mice in the TBI group had abnormal morphologies, characterized by mitochondrial

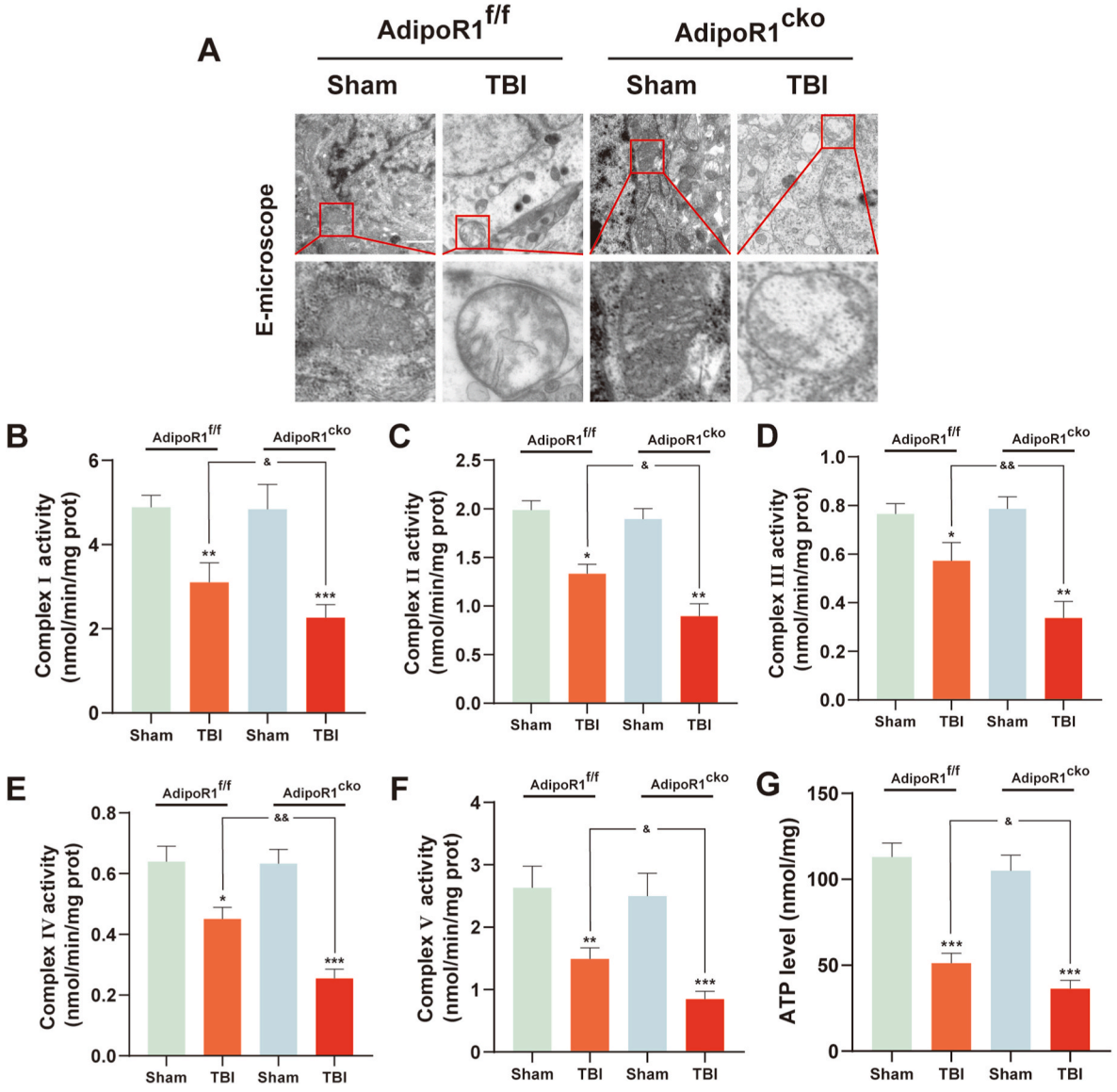

Fig. 4. Mitochondrial damage were aggravated by neuron-specific AdipoR1 conditional knockout after TBI. (A) Representative ultrastructure of neurons and enlarged mitochondrial ultrastructure in each group. Scale bar: 1 μm. (B–F) Effects of AdipoR1 knockout on levels of the mitochondrial respiratory chain complexes I, II, III, IV, and V. (G) Effects of AdipoR1 knockout on ATP levels. Data are presented as mean ± SD for n = 6. *p < 0.05, **p < 0.01 and ***p < 0.001 vs sham group in each strain of mice, $^{\&}$p < 0.05, $^{\&\&}$p < 0.01.

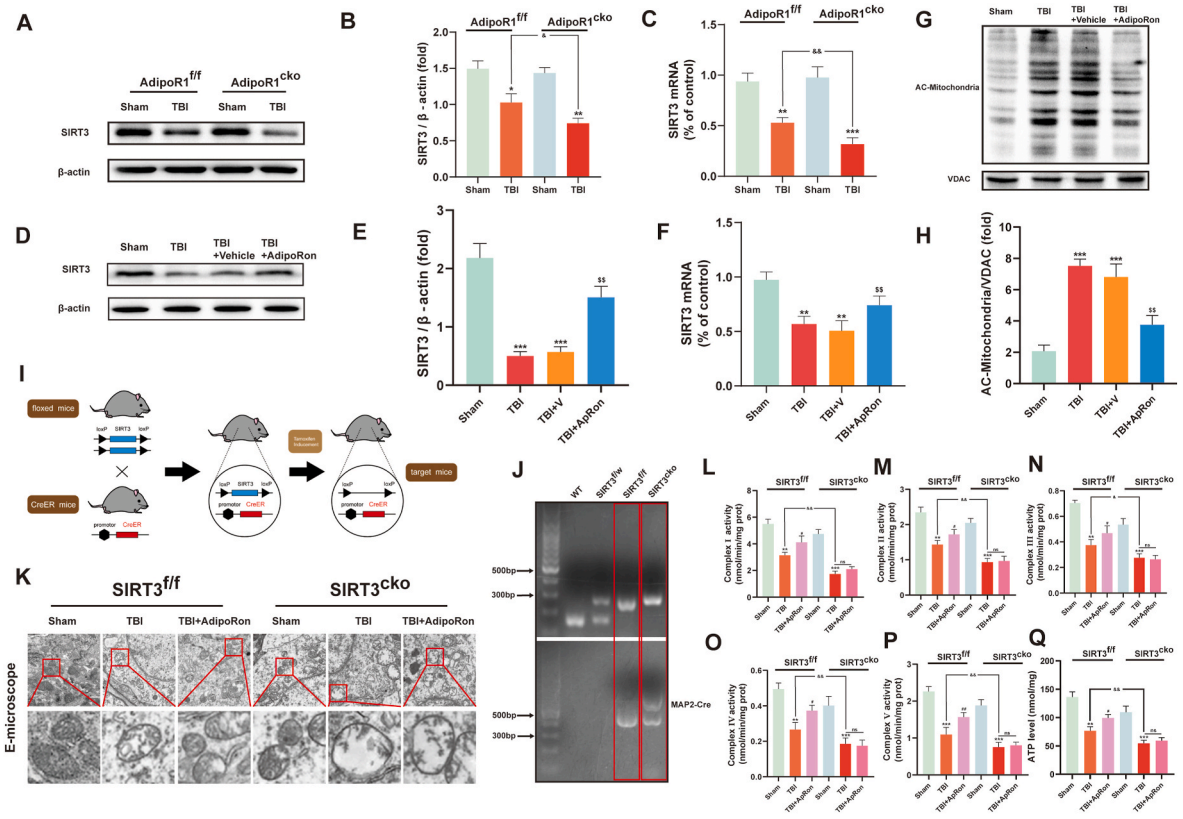

Fig. 5. APN/AdipoR1 signaling exerts mitochondrial protection effects after TBI by regulating SIRT3. (A, B) Western blot results and corresponding statistical analysis of SIRT3 expressions. (C) PCR results for the effects of AdipoR1 knockout on SIRT3 transcription after TBI. *$p < 0.05$, **$p < 0.01$ and ***$p < 0.001$ vs sham group in each strain of mice, $^{\&}p < 0.05$, $^{\&\&}p < 0.01$. (D, E) Western blot and statistical analysis of SIRT3 levels. (F) PCR results for the effects of AdipoRon treatment on SIRT3 transcription after TBI. (G, H) Western blot and statistical analysis of the acetylation levels of the mitochondrial protein. **$p < 0.01$ and ***$p < 0.001$ vs sham group, $^{\$\$}p < 0.01$ vs TBI + vehicle group. (I) Construction of SIRT3 conditional knockout models. (J) Identification results of the neuron-specific SIRT3 conditional knockout mice. (K) Representative ultrastructure of neurons and enlarged mitochondrial ultrastructure in each group. Scale bar: 1 μm. (L–P) Effects of SIRT3 knockout on the levels of mitochondrial respiratory chain complexes I, II, III, IV, and V. (Q) ATP levels in each group. Data are presented as mean ± SD for n = 6. **$p < 0.01$ and ***$p < 0.001$ vs sham group in each strain of mice, $^{\#}p < 0.05$ and $^{\#\#}p < 0.01$ vs TBI group in each strain of mice, $^{\&}p < 0.05$, $^{\&\&}p < 0.01$, ns: no statistical significance.

swelling and loss as well as disruption of the mitochondrial cristae and mitochondrial membrane integrity (Fig. 5K). However, compared to $SIRT3^{flox/flox}$ mice, impairments of mitochondrial morphologies in $SIRT3^{CKO}$ mice were exacerbated after TBI (Fig. 5K). Pathological changes in mitochondria from $SIRT3^{flox/flox}$ mice were partially reversed by AdipoRon treatment after TBI (Fig. 5K). This beneficial effect was undetectable in $SIRT3^{CKO}$ mice (Fig. 5K). To elucidate if APN/AdipoR1 signaling exerts its effects on mitochondrial functions through SIRT3, we analyzed mitochondrial respiratory chain complexes I, II, III, IV, and V activities and ATP levels. It was found that SIRT3 deletion decreased the activities of complexes I, II, III, IV, and V as well as ATP levels after TBI, and AdipoRon treatment could only exert its protective effects in $SIRT3^{flox/flox}$ mice (Fig. 5L–Q). These results indicate that the protective effect of APN/AdipoR1 signaling on neuronal mitochondrial morphology and function after TBI are likely SIRT3-dependent.

3.8. APN/AdipoR1 signaling plays an anti-oxidant stress role after TBI through the SIRT3/PRDX3 axis

We evaluated whether the protective effects of APN/AdipoR1 signaling on TBI-induced oxidative stress also rely on SIRT3. It was found that TBI-induced increase in DHE fluorescence intensities and MDA levels were exacerbated in $SIRT3^{CKO}$ mice, compared to $SIRT3^{flox/flox}$ mice (Fig. 6A–C). Although AdipoRon treatment rescued the increase in DHE fluorescence intensity and MDA levels in $SIRT3^{flox/flox}$ mice, it did not reverse this trend in $SIRT3^{CKO}$ mice (Fig. 6A–C). Compared to $SIRT3^{flox/flox}$ mice, $SIRT3^{CKO}$ mice exhibited suppressed MnSOD and GSH-Px levels after TBI (Fig. 6D and E). Meanwhile, the TBI-mediated decrease in MnSOD and GSH-Px levels in $SIRT3^{flox/flox}$ mice was reversed by AdipoRon treatment, however, upon SIRT3 loss, these effects were not rescued by AdipoRon treatment (Fig. 6D and E). The above-described results demonstrate that APN/AdipoR1 signaling protects against oxidative stress by modulating the functions of SIRT3, and SIRT3 affects the functions of substrate proteins via deacetylation. To further elucidate the antioxidant mechanism of APN/SIRT3 signaling axis, we found Peroxiredoxin 3 (PRDX3), the most abundant and efficient peroxidase in mitochondria, plays an important role in this process. Both previous literature reports [35] and the results of our experiment have been pointing to the important role of PRDX3 in anti-oxidative stress correlated with SIRT3. By culturing primary cortical neurons from $SIRT3^{flox/flox}$ mice, we generated an *in vitro* cell-based model. Primary neurons were infected with Cre-recombinase adenovirus (Ad-Cre-GFP) to genetically knock out SIRT3 (Fig. 6F). Specifically, PRDX3 acetylation levels were elevated after scratch treatment, which mimics *in vitro* TBI in both cell lines. AdipoRon could only suppress PRDX3 acetylation levels in $SIRT3^{flox/flox}$ primary neurons (Fig. 6G and H). And SIRT3 can directly interact with PRDX3 through protein-protein interactions (Fig. 6I and J). Then, we investigated the roles of PRDX3 in APN/AdipoR1 signaling-mediated anti-oxidative stress effects. Both mitochondrial ROS and MDA levels were significantly increased after scratch treatment, however, AdipoRon treatment reversed these outcomes (Fig. 6K-M). Conversely, in PRDX3 knockdown

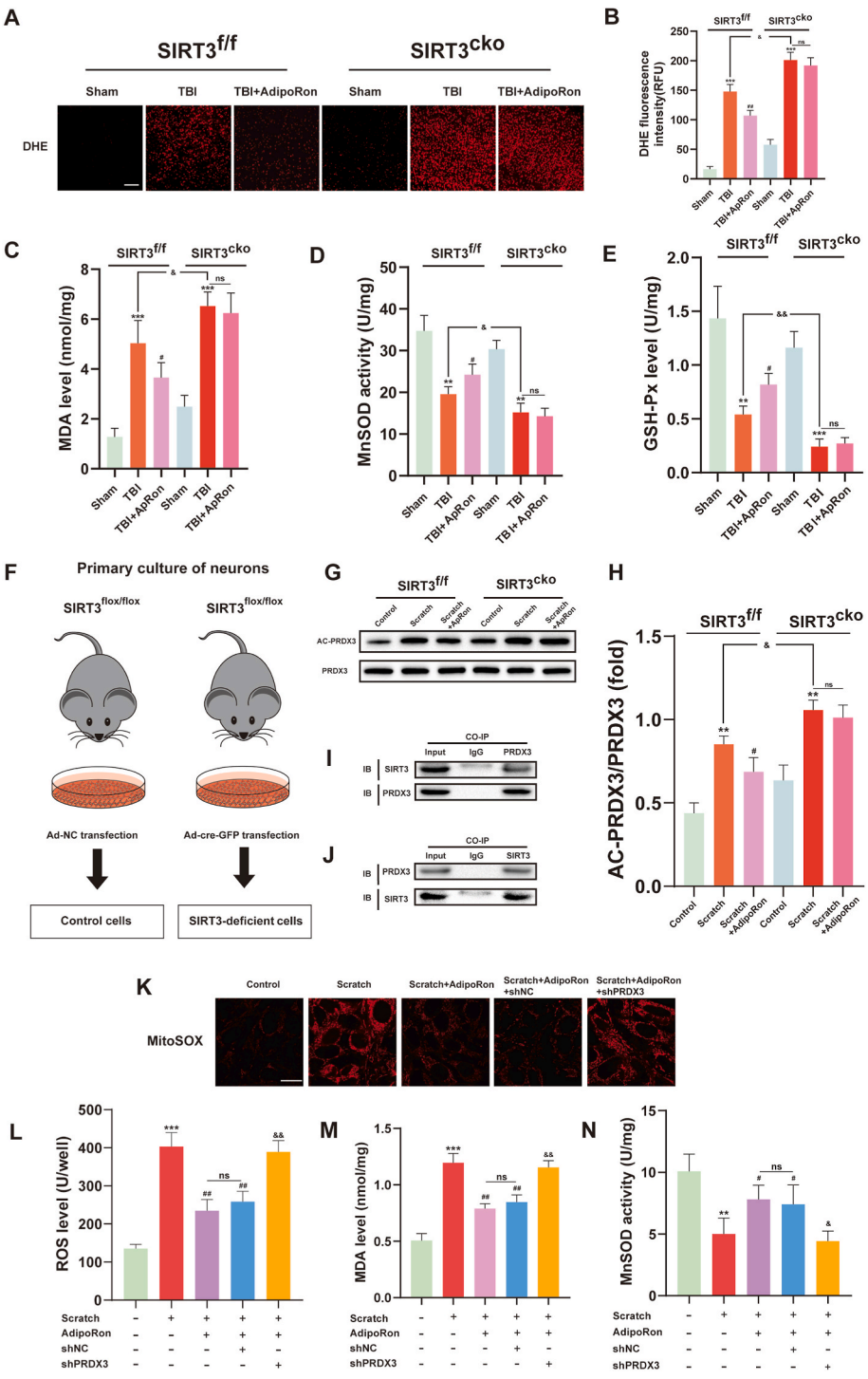

Fig. 6. APN/AdipoR1 signaling exerts anti-oxidative stress effects via the SIRT3/PRDX3 axis after TBI. (A, B) Representative DHE images and statistical analysis of DHE fluorescence intensities for perilesional cortex 24 h after TBI, which indicates ROS levels. Scale bar: 100 μm. (C–E) Effects of SIRT3 knockout and AdipoRon treatment on MnSOD activities as well as MDA and GSH-Px levels. $^{**}p < 0.01$ and $^{***}p < 0.001$ vs sham group in each strain of mice, $^{\#}p < 0.05$ and $^{\#\#}p < 0.01$ vs TBI group in each strain of mice, $^{\&}p < 0.05$, $^{\&\&}p < 0.01$, ns: no statistical significance. (F) Experimental design for generating SIRT3 conditional knockout primary neurons. (G, H) Representative Western blot and statistical analysis of acetylation levels of PRDX3 after TBI. $^{**}p < 0.01$ vs control group in each strain of cells, $^{\#}p < 0.05$ vs scratch group in each strain of cells, $^{\&}p < 0.05$, ns: no statistical significance. (I, J) CoIP of PRDX3 with SIRT3 and SIRT3 with PRDX3. Input represents total protein used for IP. IP, immunoprecipitation; IB, immunoblotting. (K, L) Representative MitoSOX images and statistical analysis of MitoSOX fluorescence intensity for the effects of PRDX3 knockdown on primary neurons, 24 h after scratch, which indicates ROS levels. Scale bar: 50 μm. (M, N) Effects of PRDX3 knockdown and AdipoRon treatment on MnSOD activities and MDA levels. Data are presented as mean ± SD for n = 6. $^{**}p < 0.01$ and $^{***}p < 0.001$ vs control group, $^{\#}p < 0.05$ and $^{\#\#}p < 0.01$ vs scratch group, $^{\&}p < 0.05$ and $^{\&\&}p < 0.01$ vs scratch + AdipoRon + shNC group, ns: no statistical significance.

group, protective effects of APN/AdipoR1 signaling were significantly weakened, compared to the scratch + AdipoRon + shNC group (Fig. 6K-M). Moreover, AdipoRon treatment remarkably restored MnSOD activities after scratch, whereas this protective effect of APN/AdipoR1 signaling was nullified in the PRDX3 knockdown group (Fig. 6N). Collectively, these results reveal that the anti-oxidative stress role of APN/AdipoR1 signaling is dependent on the SIRT3/PRDX3 axis.

3.9. Neuron-specific SIRT3 conditional knockout abolished the cerebral protective effects of APN/AdipoR1 signaling after TBI

We evaluated the effects of SIRT3 on brain injury after TBI using $SIRT3^{CKO}$ mice. Upon SIRT3 knockout, TBI-induced cerebral lesion volumes and neurological deficits were significantly exacerbated (Fig. 7A–E). AdipoRon treatment could only mitigate these impairments in $SIRT3^{flox/flox}$ mice (Fig. 7A–E). TBI-induced apoptotic cells in $SIRT3^{CKO}$ mice increased compared with those in $SIRT3^{flox/flox}$ mice and activation of APN/AdipoR1 signaling could only reduce the apoptotic cells in $SIRT3^{flox/flox}$ mice (Fig. 7F and G). Apoptosis biomarker levels in $SIRT3^{flox/flox}$ mice showed that after TBI, the decrease in antiapoptotic proteins (Bcl-2) and the increase in apoptotic cells and the proapoptotic protein (Bax) were moderately alleviated by AdipoRon treatment; This action was undetectable in $SIRT3^{CKO}$ mice (Fig. 7H–J). Therefore, SIRT3 plays a prominent role in protective effects of APN/AdipoR1 signaling

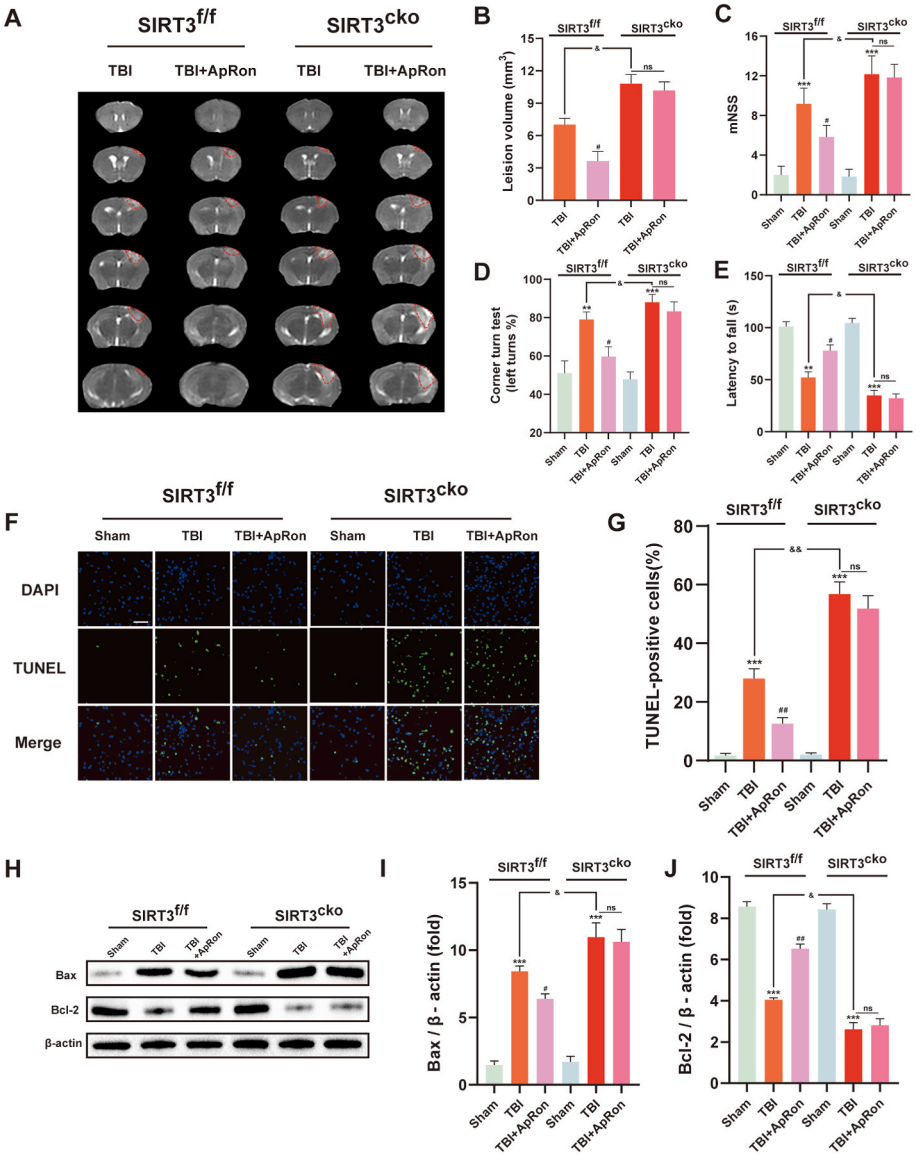

Fig. 7. Cerebral protective effects of APN/AdipoR1 signaling were offset by neuron-specific SIRT3 conditional knockout after TBI. (A, B) Representative MRI images and statistical analysis of lesion volumes for mice brains 24 h after TBI. (C–E) Effects of APN knockout and AdipoRon treatment on neurological functional deficit scores 24 h after TBI. (F, G) Representative images of TUNEL staining 24 h after TBI and corresponding statistical analysis ha. Scale bar: 100 μm. (H–J) Representative Western blot and statistical analysis of Bcl-2 and Bax protein levels. Data are presented as mean ± SD for n = 6. $^{**}p < 0.01$ and $^{***}p < 0.001$ vs sham group in each strain of mice, $^{\#}p < 0.05$ and $^{\#\#}p < 0.01$ vs TBI group in each strain of mice, $^{\&}p < 0.05$, $^{\&\&}p < 0.01$, ns: no statistical significance.

against TBI-induced brain damage.

3.10. *Activated APN/AdipoR1 signaling restores SIRT3 transcription and expressions via AMPK/PGC-1α pathway after TBI*

Further, the internal mechanism by which APN/AdipoR1 signaling regulates SIRT3 was investigated. Activation of APN/AdipoR1 signaling significantly improved the transcription levels of SIRT3 after TBI. We hypothesized that AdipoR1 affects SIRT3 transcription. However, AdipoR1 is a membrane receptor, therefore, how does AdipoR1 regulate SIRT3 transcription? The AMPK pathway is the classical downstream of AdipoR1, which has been demonstrated to promote PGC-1α expressions, a crucial upstream transcription factor of SIRT3. We postulate that SIRT3 synthesis is affected by APN/AdipoR1 signaling via the AdipoR1/AMPK/PGC-1α signaling pathway. First, this postulate was evaluated using AdipoR1CKO mice. It was found that SIRT3 mRNA and AMPK phosphorylation levels as well as PGC-1α and SIRT3 expressions were significantly reduced in both AdipoR1flox/flox mice and AdipoR1CKO mice after TBI (Fig. 8A–E). This reduction was more prominent in AdipoR1CKO mice and could only be reversed by AdipoRon treatment in AdipoR1flox/flox mice (Fig. 8A–E). Upon AMPK phosphorylation inhibition using compound C, AdipoRon could not restore SIRT3 mRNA and AMPK phosphorylation levels as well as PGC-1α and SIRT3 expressions after scratch (Fig. 8F–I). Based on the above findings, APN/AdipoR1 signaling exerts its protective effects on neurons by triggering the AdipoR1/AMPK/PGC-1α pathway, which activates SIRT3 transcription and subsequently enriches SIRT3 within the mitochondria.

As the diagram illustrates in Fig. 8J, our findings suggest that APN/AdipoR1 axis protects against the oxidative stress and relieves the neuronal apoptosis under the conditions of TBI. This mechanism relies on SIRT3-mediated mitochondrial homeostasis and antioxidant system. Collectively, we demonstrate neuroprotective effects of activation of APN/AdipoR1/SIRT3 signaling which make it as a promising target for disease-modifying therapy for TBI.

4. Discussion

Death and disability rates from TBI remain very high [64]. Unfortunately, there are no effective pharmacotherapies for TBI patients, resulting in poor prognostic outcomes and high disability rates [65,66]. APN is a putative key modulator of CNS homeostasis [67–69]. However, it has not been determined whether APN can protect the CNS from TBI. Our findings can be summarized as: i. Activation of APN/AdipoR1 signaling exerts protective effects in the TBI process. ii. Activation of

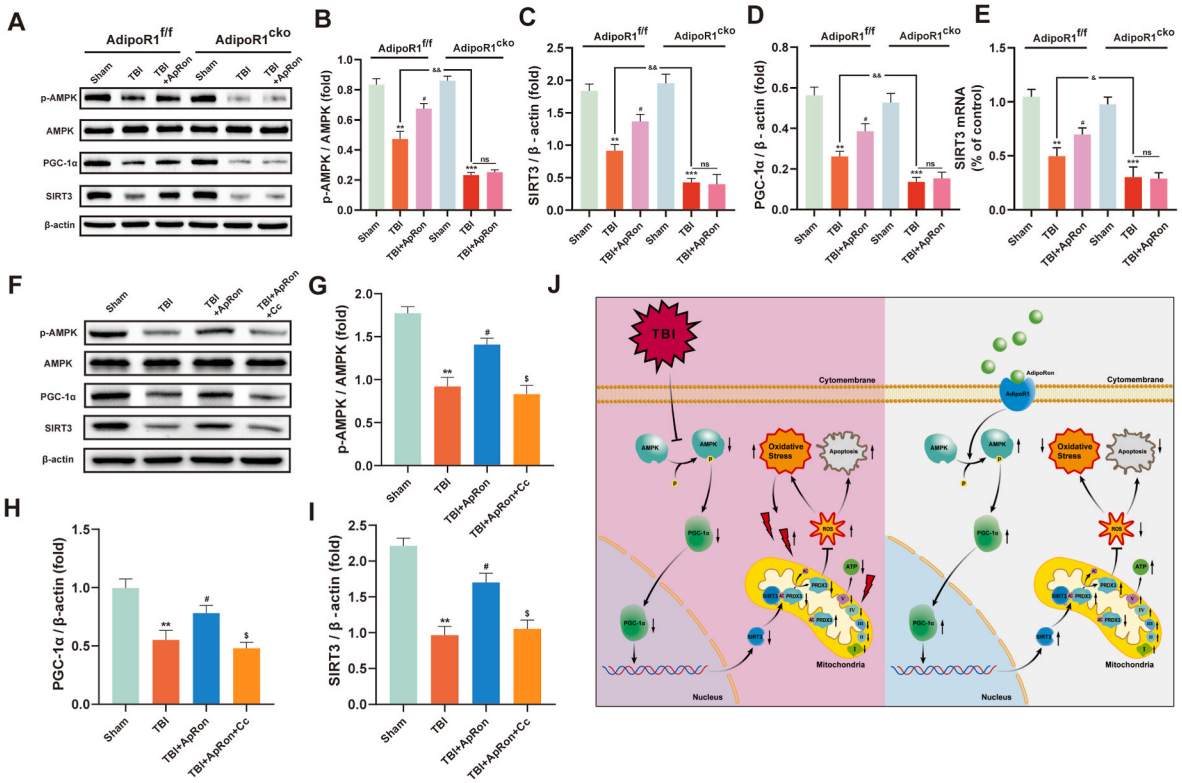

Fig. 8. Transcription and expressions of SIRT3 were regulated by AdipoR1/AMPK/PGC-1α signaling pathway in TBI models. (A–D) Western blot and statistical analysis of the phosphorylation of AMPK and expressions of SIRT3 and PGC-1α. (E) The transcription results of SIRT3 in AdipoR1$^{flox/flox}$ and AdipoR1^{CKO} mice. **$p < 0.01$ and ***$p < 0.001$ vs sham group in each strain of mice, $^{\#}p < 0.05$ vs TBI group in each strain of mice, $^{\&}p < 0.05$, $^{\&\&}p < 0.01$, ns: no statistical significance. (F–I) Effects of AMPK phosphorylation inhibitor and AdipoRon treatment on AMPK phosphorylation and expressions of SIRT3 and PGC-1α after TBI. (J) Mechanism involved in protective effects of activated APN/AdipoR1 signaling after TBI. Data are presented as mean ± SD for n = 6. **$p < 0.01$ vs sham group, $^{\#}p < 0.05$ vs TBI group, $^{\$}p < 0.05$ vs TBI + AdipoRon group.

APN/AdipoR1 signaling can significantly mitigate TBI-induced mitochondrial injury and oxidative stress; ii. The neuroprotective effects of APN/AdipoR signaling are exerted by modulation of SIRT3-mediated protective effects on the mitochondria; iv. PRDX3 is a vital target of the APN/SIRT3 axis in anti-oxidative stress; v. The AdipoR1/AMPK/PGC-1α pathway is an intrinsic regulatory mechanism of APN that is involved in promoting SIRT3 transcription.

Biologically, through its anti-inflammatory, anti-oxidative, and anti-apoptotic properties, APN exerts neuroprotective effects in various diseases, such as atherosclerosis, myocardial ischemia, myocardial infarction and in various CNS diseases [29,70–75]. But, the role of APN on TBI has not been established. We found that APN deficiency exacerbates TBI-induced lesion volume, brain edema, neurological functional deficits, oxidative stress and apoptosis, indicating a correlation between APN levels and the TBI process. We further investigated whether APN/AdipoR signaling activation has protective functions against TBI. Activated APN/AdipoR signaling significantly reduced brain tissue damage, neurological function deficits, and alleviated oxidative stress as well as neural apoptosis after TBI. These findings elucidate on the effects of APN in CNS diseases. Several studies have shown that APN protects against ischemic stroke, ICH and Alzheimer's disease (AD) [29,70,74]. Further, APN/AdipoR signaling was found to play a protective role in preventing TBI progression. This provides an experimental basis for APN to be applied in treatment of TBI. Biologically, APN primarily acts through two receptors: AdipoR1 and AdipoR2, which are ubiquitously expressed in neural cells [26,27]. To identify which AdipoR is responsible for the protective effects of APN/AdipoR signaling pathway, adenoviral-mediated shRNAs were used to knock down AdipoR1 and AdipoR2. AdipoR1 deficiency abolished the cerebroprotective effects of APN/AdipoR signaling.

Transmission electron micrographs revealed that mitochondrial damage was more severe in AdipoR1^{CKO} mice than in AdipoR1$^{flox/flox}$ mice after TBI. Since the mitochondria is the main source of cellular ATP and plays an essential role in cell survival, growth, metabolism, oxidative injury, and apoptosis, mitochondrial dysfunction is a common feature of many diseases [76–81]. Further, we investigated the potential mechanisms of APN/AdipoR1 signaling on the mitochondria. Since SIRT3 is exclusively located in the mitochondria [82], it plays an important role in regulating mitochondrial functions, metabolism, antioxidative defense systems as well as energy metabolism [40,41,43,46]. SIRT3 is primarily expressed in neurons [31,82]. After TBI, we found suppressed SIRT3 levels, which were restored upon APN/AdipoR1 signaling activation. We postulate that SIRT3 is key in the regulatory role of APN/AdipoR1 signaling in mitochondrial morphology and function. The protective effects of AdipoRon on mitochondrial morphology and function were ameliorated by SIRT3 knockout. Correspondingly, the effects of AdipoRon against oxidative stress and apoptosis were SIRT3 dependent. Therefore, APN/AdipoR1 signaling regulates mitochondrial morphology and functions through SIRT3 modulation. Given the important role of APN/AdipoR1 signaling and SIRT3 in metabolic diseases and other organ diseases, elucidation of this new mechanism may be generalized to other diseases.

To clarify the antioxidant mechanisms of the APN/SIRT3 signaling axis, we found that PRDX3, the most abundant and efficient peroxidase in the mitochondria [35], plays an important role in this process. PRDX3 has a major role in controlling mitochondrial ROS production and ameliorating oxidative stress [35,83,84]. Acetylation levels of PRDX3 after TBI were markedly increased. Even though APN could not affect PRDX3 expressions, it significantly suppressed PRDX3 acetylation levels. This effect is dependent on normal deacetylation functions of

SIRT3. We also demonstrated that PRDX3 deficiency ameliorated anti-oxidative stress and anti-apoptosis actions of APN/AdipoR1 signaling. Our findings revealed that deacetylated PRDX3 by SIRT3 is essential for anti-oxidative stress and anti-apoptosis effects of APN/AdipoR1 signaling.

Then, we explored the internal mechanisms through which APN/AdipoR1 signaling regulates SIRT3. Activation of APN/AdipoR1 signaling significantly improved the transcription levels of SIRT3 after TBI. We hypothesized that AdipoR1 affects SIRT3 transcriptions. However, AdipoR1 is a membrane receptor, therefore, how does it regulate SIRT3 transcription? The AMPK pathway is the classical downstream of AdipoR1, which has been demonstrated to promote expressions of PGC-1α, a crucial upstream transcription factor of SIRT3. We postulate that SIRT3 synthesis is affected by APN/AdipoR1 signaling via the AdipoR1/AMPK/PGC-1α signaling pathway. This hypothesis was validated via a series of experiments involving AdipoR1^{CKO} mice and the AMPK inhibitor. Transcription and expressions of SIRT3 were found to be regulated by the AdipoR1/AMPK/PGC-1α signaling pathway.

This study is associated with some limitations. First, we investigated the protective mechanisms of APN/AdipoR1 signaling against early brain damage after TBI, however, its role in advanced brain injury remains unclear. Studies should assess the long-term effects of APN/AdipoR1 signaling. Second, there is a need to analyze correlations between plasma APN levels in TBI patients and prognostic outcomes of TBI patients to substantiate the translational value of AdipoRon, which provides a basis for future clinical applications of AdipoRon in TBI treatment.

In conclusion, the APN/AdipoR signaling pathway plays its roles by activating AdipoR1, which subsequently helps to increase SIRT3 expression and promote the restoration of mitochondrial anti-oxidative ability. Ultimately, the effects of APN/AdipoR1 signaling in anti-oxidative stress, anti-apoptosis and preventing TBI are achieved.

Declaration of competing interests

The authors declare that they have no conflicts of interest.

Acknowledgements

This study was supported by the State Key Program of the National Natural Science Foundation of China (Nos. 81630027 and 82130038). Thanks to Clinical Research Center for Neurosurgical Diseases of Shaanxi Province and Shaanxi International Science & Technology Cooperation Base for their support.

References

[1] M. Vaninetti, et al., fMRI findings in MTBI patients with headaches following rTMS, Sci. Rep. 11 (1) (2021) 9573.
[2] A.G. Mustafa, et al., Mitochondrial protection after traumatic brain injury by scavenging lipid peroxyl radicals, J. Neurochem. 114 (1) (2010) 271–280.
[3] C.L. H Huang, H. Huang, Clinical neurorestorative progress in traumatic brain injury, J. Neurorestoratol. 3 (2015) 57–62.
[4] H. Wang, et al., Aucubin alleviates oxidative stress and inflammation via Nrf2-mediated signaling activity in experimental traumatic brain injury, J. Neuroinflammation 17 (1) (2020) 188.
[5] L.S. Chiu, et al., Effect of polyarginine peptide R18D following a traumatic brain injury in sprague-dawley rats, Curr. Ther. Res. Clin. Exp. 92 (2020), 100584.
[6] M.I. Betancur, et al., Chondroitin sulfate glycosaminoglycan matrices promote neural stem cell maintenance and neuroprotection post-traumatic brain injury, ACS Biomater. Sci. Eng. 3 (3) (2017) 420–430.
[7] W.L. Talley, et al., Methylene blue is neuroprotective against mild traumatic brain injury, J. Neurotrauma 31 (11) (2014) 1063–1071.
[8] Z. Sun, et al., VX765 attenuates pyroptosis and HMGB1/TLR4/NF-kappaB pathways to improve functional outcomes in TBI mice, Oxid. Med. Cell. Longev. 2020 (2020), 7879629.
[9] T. Zhao, J. Zhao, Genetic effects of adiponectin on blood lipids and blood pressure, Clin. Endocrinol. 74 (2) (2011) 214–222.
[10] A. Doria, Genetics of diabetes complications, Curr. Diabetes Rep. 10 (6) (2010) 467–475.
[11] I.K. Lee, et al., PEG-BHD1028 peptide regulates insulin resistance and fatty acid beta-oxidation, and mitochondrial biogenesis by binding to two heterogeneous binding sites of adiponectin receptors, AdipoR1 and AdipoR2, Int. J. Mol. Sci. 22 (2) (2021).
[12] P. Bobbert, et al., Adiponectin expression in patients with inflammatory cardiomyopathy indicates favourable outcome and inflammation control, Eur. Heart J. 32 (9) (2011) 1134–1147.
[13] H. Liu, et al., Adiponectin peptide alleviates oxidative stress and NLRP3 inflammasome activation after cerebral ischemia-reperfusion injury by regulating AMPK/GSK-3 beta, Exp. Neurol. 329 (2020), 113302.
[14] J. Jortay, et al., Local induction of adiponectin reduces lipopolysaccharide-triggered skeletal muscle damage, Endocrinology 151 (10) (2010) 4840–4851.
[15] W. Song, et al., Therapeutic window of globular adiponectin against cerebral ischemia in diabetic mice: the role of dynamic alteration of adiponectin/adiponectin receptor expression, Sci. Rep. 5 (2015), 17310.
[16] J. Park, et al., Gene-gene interaction analysis identifies a new genetic risk factor for colorectal cancer, J. Biomed. Sci. 22 (2015) 73.
[17] S. Fukuda, et al., Systemic arteriosclerosis and eating behavior in Japanese type 2 diabetic patients with visceral fat accumulation, Cardiovasc. Diabetol. 14 (2015) 8.
[18] J. Shang, et al., Different associations of plasma biomarkers in Alzheimer's disease, mild cognitive impairment, vascular dementia, and ischemic stroke, J. Clin. Neurol. 14 (1) (2018) 29–34.
[19] S.P. Efstathiou, et al., Plasma adiponectin levels and five-year survival after first-ever ischemic stroke, Stroke 36 (9) (2005) 1915–1919.
[20] N. Ilhan, et al., The emerging role of leptin, Adiponectin and Visfatin in Ischemic/Hemorrhagic stroke, Br. J. Neurosurg. 33 (5) (2019) 504–507.
[21] R.C. Ng, et al., Chronic adiponectin deficiency leads to Alzheimer's disease-like cognitive impairments and pathologies through AMPK inactivation and cerebral insulin resistance in aged mice, Mol. Neurodegener. 11 (1) (2016) 71.
[22] X. Wu, et al., Recombinant adiponectin peptide promotes neuronal survival after intracerebral haemorrhage by suppressing mitochondrial and ATF4-CHOP apoptosis pathways in diabetic mice via Smad 3 signalling inhibition, Cell Prolif 53 (2) (2020), e12759.
[23] Q. Zhang, et al., Critical role of AdipoR1 in regulating Th17 cell differentiation through modulation of HIF-1alpha-Dependent glycolysis, Front. Immunol. 11 (2020) 2040.
[24] N. Smolinska, et al., Transcriptomic analysis of porcine endometrium during implantation after in vitro stimulation by adiponectin, Int. J. Mol. Sci. 20 (6) (2019).
[25] H.S. Park, et al., Resveratrol increases AdipoR1 and AdipoR2 expression in type 2 diabetic nephropathy, J. Transl. Med. 14 (1) (2016) 176.
[26] M. Okada-Iwabu, et al., A small-molecule AdipoR agonist for type 2 diabetes and short life in obesity, Nature 503 (7477) (2013) 493–499.
[27] X. Wu, et al., An adiponectin receptor agonist reduces type 2 diabetic periodontitis, J. Dent. Res. 98 (3) (2019) 313–321.
[28] W. Miao, et al., Adiponectin ameliorates hypoperfusive cognitive deficits by boosting a neuroprotective microglial response, Prog. Neurobiol. 205 (2021), 102125.
[29] X. Li, et al., Adiponectin attenuates NADPH oxidase-mediated oxidative stress and neuronal damage induced by cerebral ischemia-reperfusion injury, Biochim. Biophys. Acta, Mol. Basis Dis. 1863 (12) (2017) 3265–3276.
[30] B. Wang, et al., Adiponectin attenuates oxygen-glucose deprivation-induced mitochondrial oxidative injury and apoptosis in hippocampal HT22 cells via the JAK2/STAT3 pathway, Cell Transplant. 27 (12) (2018) 1731–1743.
[31] Y. Cen, D.Y. Youn, A.A. Sauve, Advances in characterization of human sirtuin isoforms: chemistries, targets and therapeutic applications, Curr. Med. Chem. 18 (13) (2011) 1919–1935.
[32] W. Yang, et al., Mitochondrial sirtuin network reveals dynamic SIRT3-dependent deacetylation in response to membrane depolarization, Cell 167 (4) (2016) 985–1000, e21.
[33] T. Zhang, et al., SIRT3 acts as a positive autophagy regulator to promote lipid mobilization in adipocytes via activating AMPK, Int. J. Mol. Sci. 21 (2) (2020).
[34] A. Vassilopoulos, et al., SIRT3 deacetylates ATP synthase F1 complex proteins in response to nutrient- and exercise-induced stress, Antioxidants Redox Signal. 21 (4) (2014) 551–564.
[35] Z. Wang, et al., SIRT3-mediated deacetylation of PRDX3 alleviates mitochondrial oxidative damage and apoptosis induced by intestinal ischemia/reperfusion injury, Redox Biol. 28 (2020), 101343.
[36] A.S. Bause, M.S. Matsui, M.C. Haigis, The protein deacetylase SIRT3 prevents oxidative stress-induced keratinocyte differentiation, J. Biol. Chem. 288 (51) (2013) 36484–36491.
[37] S. Dikalov, et al., Tobacco smoking induces cardiovascular mitochondrial oxidative stress, promotes endothelial dysfunction, and enhances hypertension, Am. J. Physiol. Heart Circ. Physiol. 316 (3) (2019) H639–H646.
[38] L.H. Mbye, et al., Attenuation of acute mitochondrial dysfunction after traumatic brain injury in mice by NIM811, a non-immunosuppressive cyclosporin A analog, Exp. Neurol. 209 (1) (2008) 243–253.
[39] I.N. Singh, P.G. Sullivan, E.D. Hall, Peroxynitrite-mediated oxidative damage to brain mitochondria: protective effects of peroxynitrite scavengers, J. Neurosci. Res. 85 (10) (2007) 2216–2223.
[40] Z. Liu, et al., Hydrogen Sulfide Protects against Paraquat-Induced Acute Liver Injury in Rats by Regulating Oxidative Stress, Mitochondrial Function, and Inflammation, vol. 2020, Oxid Med Cell Longev, 2020, 6325378.
[41] A.B. Potthast, et al., Impact of nutrition on short-term exercise-induced sirtuin regulation: vegans differ from omnivores and lacto-ovo vegetarians, Nutrients 12 (4) (2020).

[42] S. Peng, et al., LCZ696 ameliorates oxidative stress and pressure overload-induced pathological cardiac remodeling by regulating the sirt3/MnSOD pathway, Oxid. Med. Cell. Longev. 2020 (2020), 9815039.
[43] M. Zhai, et al., Melatonin ameliorates myocardial ischemia reperfusion injury through SIRT3-dependent regulation of oxidative stress and apoptosis, J. Pineal Res. 63 (2) (2017).
[44] L. Liu, et al., Melatonin protects against focal cerebral ischemia-reperfusion injury in diabetic mice by ameliorating mitochondrial impairments: involvement of the Akt-SIRT3-SOD2 signaling pathway, Aging (Albany NY) 13 (12) (2021) 16105–16123.
[45] H. Zeng, J.X. Chen, Microvascular rarefaction and heart failure with preserved ejection fraction, Front Cardiovasc Med 6 (2019) 15.
[46] N. Zhang, et al., Mitochondrial respiratory chain and its regulatory elements SIRT1 and SIRT3 play important role in the initial process of energy conversion after moxibustion at local skin, Evid Based Complement Alternat Med 2020 (2020), 2343817.
[47] T. Chen, et al., The AMPAR antagonist perampanel protects the neurovascular unit against traumatic injury via regulating Sirt3, CNS Neurosci. Ther. 27 (1) (2021) 134–144.
[48] Q. Yang, et al., Will sirtuins Be promising therapeutic targets for TBI and associated neurodegenerative diseases? Front. Neurosci. 14 (2020) 791.
[49] W. Cui, et al., 20-HETE synthesis inhibition attenuates traumatic brain injury-induced mitochondrial dysfunction and neuronal apoptosis via the SIRT1/PGC-1alpha pathway: a translational study, Cell Prolif 54 (2) (2021), e12964.
[50] Y. Deng-Bryant, et al., Neuroprotective effects of tempol, a catalytic scavenger of peroxynitrite-derived free radicals, in a mouse traumatic brain injury model, J. Cerebr. Blood Flow Metabol. 28 (6) (2008) 1114–1126.
[51] D. Weber-Adrian, et al., Strategy to enhance transgene expression in proximity of amyloid plaques in a mouse model of Alzheimer's disease, Theranostics 9 (26) (2019) 8127–8137.
[52] P. Yu, et al., Progesterone-mediated angiogenic activity of endothelial progenitor cell and angiogenesis in traumatic brain injury rats were antagonized by progesterone receptor antagonist, Cell Prolif 50 (5) (2017).
[53] C. Canugovi, et al., Increased mitochondrial NADPH oxidase 4 (NOX4) expression in aging is a causative factor in aortic stiffening, Redox Biol. 26 (2019), 101288.
[54] J.H. Seo, et al., Environmental enrichment attenuates oxidative stress and alters detoxifying enzymes in an A53T alpha-synuclein transgenic mouse model of Parkinson's disease, Antioxidants 9 (10) (2020).
[55] Z. Galehdar, et al., Neuronal apoptosis induced by endoplasmic reticulum stress is regulated by ATF4-CHOP-mediated induction of the Bcl-2 homology 3-only member PUMA, J. Neurosci. 30 (50) (2010) 16938–16948.
[56] K.W. Chung, et al., Mitochondrial damage and activation of the STING pathway lead to renal inflammation and fibrosis, Cell Metabol. 30 (4) (2019) 784–799, e5.
[57] Y.H. Bae, et al., Brain injury induces HIF-1alpha-dependent transcriptional activation of LRRK2 that exacerbates brain damage, Cell Death Dis. 9 (11) (2018) 1125.
[58] X. Wu, et al., Acrolein aggravates secondary brain injury after intracerebral hemorrhage through drp1-mediated mitochondrial oxidative damage in mice, Neurosci. Bull. 36 (10) (2020) 1158–1170.
[59] K. Otsu, et al., Concentration-dependent inhibition of angiogenesis by mesenchymal stem cells, Blood 113 (18) (2009) 4197–4205.
[60] Y. Zhu, et al., SS-31 Provides Neuroprotection by Reversing Mitochondrial Dysfunction after Traumatic Brain Injury, vol. 2018, Oxid Med Cell Longev, 2018, 4783602.
[61] E. Sidorova-Darmos, R. Sommer, J.H. Eubanks, The role of SIRT3 in the brain under physiological and pathological conditions, Front. Cell. Neurosci. 12 (2018) 196.
[62] R.M. Parodi-Rullan, X.R. Chapa-Dubocq, S. Javadov, Acetylation of mitochondrial proteins in the heart: the role of SIRT3, Front. Physiol. 9 (2018) 1094.
[63] L.B. Sullivan, N.S. Chandel, Mitochondrial reactive oxygen species and cancer, Cancer Metabol. 2 (2014) 17.
[64] H.W. Caplan, et al., Human cord blood-derived regulatory T-cell therapy modulates the central and peripheral immune response after traumatic brain injury, Stem Cells Transl Med 9 (8) (2020) 903–916.
[65] A. Filipek, W. Lesniak, S100A6 and its brain ligands in neurodegenerative disorders, Int. J. Mol. Sci. 21 (11) (2020).
[66] H. Xu, et al., The polarization states of microglia in TBI: a new paradigm for pharmacological intervention, Neural Plast. 2017 (2017), 5405104.
[67] N. Kubota, et al., Adiponectin stimulates AMP-activated protein kinase in the hypothalamus and increases food intake, Cell Metabol. 6 (1) (2007) 55–68.
[68] Q. Tian, et al., Hydrogen sulfide antagonizes chronic restraint stress-induced depressive-like behaviors via upregulation of adiponectin, Front. Psychiatr. 9 (2018) 399.
[69] T. Hillemacher, et al., Increased levels of adiponectin and resistin in alcohol dependence–possible link to craving, Drug Alcohol Depend. 99 (1–3) (2009) 333–337.
[70] L. Letra, et al., Adiponectin and sporadic Alzheimer's disease: clinical and molecular links, Front. Neuroendocrinol. 52 (2019) 1–11.
[71] F. Song, et al., Association of adipocytokines with carotid intima media thickness and arterial stiffness in obstructive sleep apnea patients, Front. Endocrinol. 11 (2020) 177.
[72] X. Yang, et al., KGF-2 and FGF-21 poloxamer 407 hydrogel coordinates inflammation and proliferation homeostasis to enhance wound repair of scalded skin in diabetic rats, BMJ Open Diabetes Res Care 8 (1) (2020).
[73] C.J. Lavie, et al., Omega-3 polyunsaturated fatty acids and cardiovascular diseases, J. Am. Coll. Cardiol. 54 (7) (2009) 585–594.
[74] X. Wu, et al., Recombinant adiponectin peptide ameliorates brain injury following intracerebral hemorrhage by suppressing astrocyte-derived inflammation via the inhibition of drp1-mediated mitochondrial fission, Transl Stroke Res 11 (5) (2020) 924–939.
[75] H. Kataoka, K. Sugie, Serum adiponectin levels between patients with Parkinson's disease and those with PSP, Neurol. Sci. 41 (5) (2020) 1125–1131.
[76] D.M. Tanase, et al., The predictive role of the biomarker kidney molecule-1 (KIM-1) in acute kidney injury (AKI) cisplatin-induced nephrotoxicity, Int. J. Mol. Sci. 20 (20) (2019).
[77] T.C. Huang, et al., Epirubicin induces apoptosis in osteoblasts through death-receptor and mitochondrial pathways, Apoptosis 23 (3–4) (2018) 226–236.
[78] A.G. Miranda-Diaz, A. Garcia-Sanchez, E.G. Cardona-Munoz, Foods with potential prooxidant and antioxidant effects involved in Parkinson's disease, Oxid. Med. Cell. Longev. 2020 (2020), 6281454.
[79] J. Lee, Mitochondrial drug targets in neurodegenerative diseases, Bioorg. Med. Chem. Lett 26 (3) (2016) 714–720.
[80] Y. Zhang, et al., The effect of extracellular vesicles on the regulation of mitochondria under hypoxia, Cell Death Dis. 12 (4) (2021) 358.
[81] L. Ni, et al., The protective effect of Bcl-xl overexpression against oxidative stress-induced vascular endothelial cell injury and the role of the Akt/eNOS pathway, Int. J. Mol. Sci. 14 (11) (2013) 22149–22162.
[82] M. Perez-Salvia, et al., Barcelona conference on epigenetics and cancer: 50 years of histone acetylation, Epigenetics 10 (5) (2015) 446–451.
[83] Z. Xu, et al., MicroRNA-383 promotes reactive oxygen species-induced autophagy via downregulating peroxiredoxin 3 in human glioma U87 cells, Exp. Ther. Med. 21 (5) (2021) 439.
[84] W.B. Wu, et al., Downregulation of peroxiredoxin-3 by hydrophobic bile acid induces mitochondrial dysfunction and cellular senescence in human trophoblasts, Sci. Rep. 6 (2016), 38946.